

Solar-radiation-maintained glacier recession on Kilimanjaro drawn from combined ice-radiation geometry modeling

Thomas Mölg

Tropical Glaciology Group, Department of Geography, University of Innsbruck, Innsbruck, Austria

Douglas R. Hardy

Climate System Research Center, Department of Geosciences, University of Massachusetts, Amherst, Massachusetts, USA

Georg Kaser

Tropical Glaciology Group, Department of Geography, University of Innsbruck, Innsbruck, Austria

Received 28 February 2003; revised 14 August 2003; accepted 22 August 2003; published 10 December 2003.

[1] In the context of investigating modern glacier recession on Kilimanjaro, which began around 1880, this study addresses the glacier regime of the vertical ice walls that typically form the margins of Kilimanjaro's summit glaciers. These walls have suffered a continuous lateral retreat during the twentieth century. To evaluate the role of solar radiation in maintaining glacier recession on Kilimanjaro, a radiation model is applied to an idealized representation of the 1880-ice cap. The combined process-based model calculates the spatial extent and geometry of the ice cap for various points in time after 1880. Support for input data and fundamental assumptions are provided by an automatic weather station that has operated on the summit's Northern Icefield since February 2000. Even in a simple climatic scenario only forced with an annual cycle of clouds, the basic evolution in spatial distribution of ice bodies on the summit is modeled well. The Northern and Southern Icefields form in characteristic east-west orientation, which verifies the basic idea behind the model. Forcing the model with further climate-related phenomena improves the results. It then additionally reproduces the Eastern Icefield, the third big ice entity on the summit. This study qualitatively demonstrates that solar radiation is the main climatic parameter maintaining modern glacier recession on Kilimanjaro summit, but also suggests that retreat on the inner ice cap margin might have been supported by a secondary energy source. The need for additional field measurements is emphasized in order to better understand the complex processes of glacier-climate interaction on Kilimanjaro. *INDEX TERMS:* 1620 Global Change: Climate dynamics (3309); 1827 Hydrology: Glaciology (1863); 3309 Meteorology and Atmospheric Dynamics: Climatology (1620); 3359 Meteorology and Atmospheric Dynamics: Radiative processes; 9305 Information Related to Geographic Region: Africa; *KEYWORDS:* tropical glaciers, Kilimanjaro, climate change, glacier retreat, solar radiation modeling

Citation: Mölg, T., D. R. Hardy, and G. Kaser, Solar-radiation-maintained glacier recession on Kilimanjaro drawn from combined ice-radiation geometry modeling, *J. Geophys. Res.*, 108(D23), 4731, doi:10.1029/2003JD003546, 2003.

1. Introduction

[2] As indicators of climate change, glaciers and their behavior are of undisputable value [Oerlemans, 2001]. The latest report of the *Intergovernmental Panel on Climate Change* [2001] again emphasizes the importance for climate research of understanding glacier-climate interactions correctly. Tropical glaciers represent a peculiar component of the global climate system, since they are located in a thermally homogenous atmosphere [Kaser *et al.*, 1996]. This makes them especially sensitive to humidity-related variables, as seasonality in tropical climate is solely caused by the annual

cycle of air humidity [Hardy *et al.*, 1998; Kaser, 2001]. At present, tropical glaciers still exist in Irian Jaya (New Guinea), East Africa, and in the South American Andes [Kaser and Osmaston, 2002]. In response to a complex combination of changes in air temperature, air humidity, precipitation, cloudiness, and incoming shortwave radiation they all suffered a continuous, strong recession over the past century, as summarized by Kaser [1999]. Around 1990 tropical glaciers covered a surface area of ca. 2,500 km², with more than 99% in the South American Andes [Kaser, 1999].

[3] Glacierization in East Africa is limited to three massifs close to the equator: Kilimanjaro (Tanzania, Kenya), Mount Kenya (Kenya), and Rwenzori (Zaire, Uganda). Glaciers in these massifs occupied a surface area of 5.4 km² around 1990 [Kaser, 1999]. Following the

general trend they have retreated drastically from the latest maximum extent since ca. 1880, which was comprehensively reported by *Hastenrath* [1984]. Details for Kilimanjaro are provided by *Hastenrath and Greischar* [1997], *Thompson et al.* [2002] and *Kaser et al.* [2003], for Mount Kenya by *Kruss and Hastenrath* [1987], *Hastenrath et al.* [1989] and *Hastenrath* [1995], and for the Rwenzori by *Kaser and Nogler* [1996], *Kaser and Osmaston* [2002] and *Mölg et al.* [2003]. In general, a strong reduction in precipitation at the end of the 19th century is the main reason for modern glacier recession in East Africa, reducing the glacier mass balance accumulation term considerably [Kruss, 1983; Hastenrath, 1984]. In addition, increased incoming shortwave radiation due to decreases in cloudiness - both effects of the drier climatic conditions - plays a decisive role for glacier retreat by increasing ablation, as demonstrated for Mount Kenya and Rwenzori [Kruss and Hastenrath, 1987; Mölg et al., 2003].

[4] These multiple effects of a drier climate, reduced precipitation and cloudiness, and increased incoming shortwave radiation, are in accordance with the climatic evolution of East Africa over the past 150 years as derived from climatic proxy data other than glaciers. These include historical accounts of lake levels [Hastenrath, 1984; Nicholson and Yin, 2001], wind and current observations in the Indian Ocean and their relationship to East African rainfall [Hastenrath, 2001], water balance models of lakes [Nicholson and Yin, 2001], and paleolimnological data [Verschuren et al., 2000]. All data indicate that modern East African climate experienced an abrupt and marked drop in air humidity around 1880. The ensuing relatively dry climate was maintained throughout the 20th century, as shown by instrumental records of annual precipitation amounts that vary only slightly during the 20th century [e.g., Rodhe and Virji, 1976; Hay et al., 2002]. Comparatively, a very humid climate prevailed in the couple of decades preceding 1880: lakes stood high, mountain glaciation was extensive, and precipitation was more abundant. In contrast to this shift in air humidity, there is no evidence of a sudden change in air temperature at the end of the 19th century [Hastenrath, 2001]. Moreover, East African long-term temperature records of the 20th century show diverse trends and do not exhibit a uniform warming signal [King'uyu et al., 2000; Hay et al., 2002].

[5] Kilimanjaro, Africa's highest mountain, is located in Tropical East Africa at the Kenya-Tanzania border ca. 370 km south of the Equator and about the same distance from the Indian Ocean (3°04'S/37°21'E). The huge stratovolcano (ca. 80 by 50 km) consists of three single peaks: Shira (4,005 m), Mawenzi (5,140 m), and Kibo (5,895 m) which is the only one to retain glaciers. The summit region of Kibo has subsided to form a caldera 1.9 by 2.4 km in diameter. Within this lies a second cone enclosing the Reusch Crater (RC) which harbors the eruption cone. Figure 1 shows Kibo and its glacier extent at four different intervals through the 20th century, and illustrates the drastic modern glacier recession. The 1912-, 1953-, and 1976- extents were determined by *Hastenrath and Greischar* [1997], while the 2000-extent was recently presented by *Thompson et al.* [2002]. On the basis of aerial photographs, total glacier surface area in 2000 is 2.6 km² [Thompson et al., 2002]. The 5,700 m-contour emphasized in Figure 1 is a

good indicator for delimiting the near-planar summit plateau. Currently, four ice entities remain on Kibo summit, all typically margined by vertical ice walls: the Northern and Southern Icefields northwest and south of RC, respectively, the smaller Eastern Icefield east of RC, and the quite small Furtwängler Glacier southwest of RC. Areal changes of the summit glaciers revealed by the map are primarily due to the strong lateral retreat of the vertical ice walls, while the surface lowering's contribution to glacier surface area change is small [Kaser et al., 2003]. Slope glaciers on Kibo do not descend - apart from one glacier on the western slope - below 5,000 m. Since February 2000 an automatic weather station (AWS) has operated on a horizontal glacier surface at the summit's Northern Icefield (Figure 1). AWS data through July 2002 show that monthly mean air temperatures only vary slightly around the annual mean of -7.1°C, and air temperatures (measured by ventilated sensors, e.g., *Georges and Kaser* [2002]) never rise above the freezing point. Precipitation falls entirely as snow, amounting to ~250 mm a⁻¹ (water equivalence). Further, incoming and reflected shortwave radiation relative to a horizontal surface, air humidity, barometric pressure, and wind speed and direction are measured. A synopsis of the first three years of measurements is provided by the www-server for the University of Massachusetts at <http://www.geo.umass.edu/climate/kibo.html>. As a result of large-scale circulation over East Africa [e.g., Griffiths, 1972], climate in the Kilimanjaro region is characterized by a bimodal distribution of rains centered on March to May (so called "long rains") and October to December (so called "short rains"), separated by two drier seasons [Basalirwa et al., 1999]. Together, the two rainy seasons account for 70–80% of annual precipitation [Coutts, 1969]. Data recorded by the AWS reflect this general character of climate very well.

2. Background and Aim of Study

[6] Although the recession of Kilimanjaro's glaciers is well documented and has been the central theme published since research on the mountain began in the late 1880s [e.g., Meyer, 1900; Klute, 1920; Geilinger, 1936; Hunt, 1947; Humphries, 1959; Downie and Wilkinson, 1972; Hastenrath, 1984; Osmaston, 1989; Hastenrath and Greischar, 1997; Thompson et al., 2002], the climatological interpretation of this recession has remained speculative. Early researchers emphasize the dual importance of limited precipitation and intense solar radiation in forcing glacier retreat on Kibo [e.g., Jäger, 1931; Geilinger, 1936], while recent reports and studies attribute the retreat to general global warming [e.g., Alverson et al., 2001; Irion, 2001; Thompson et al., 2002]. Connecting glacier retreat on Kilimanjaro with globally increasing air temperatures has recently attracted both scientific and public interest but is a highly simplified view as *Kaser et al.* [2003] show in a new study. From a synopsis of (i) both proxy and instrumental climate data, and (ii) observations and interpretations made during several periods of fieldwork on Kibo, they reconstruct an alternative scenario of modern glacier retreat on Kilimanjaro, based on the current understanding of physical processes at the ice-atmosphere interface. This scenario offers a working hypothesis with a much more complex view of the retreating glaciers of Kibo. Taking this complexity into

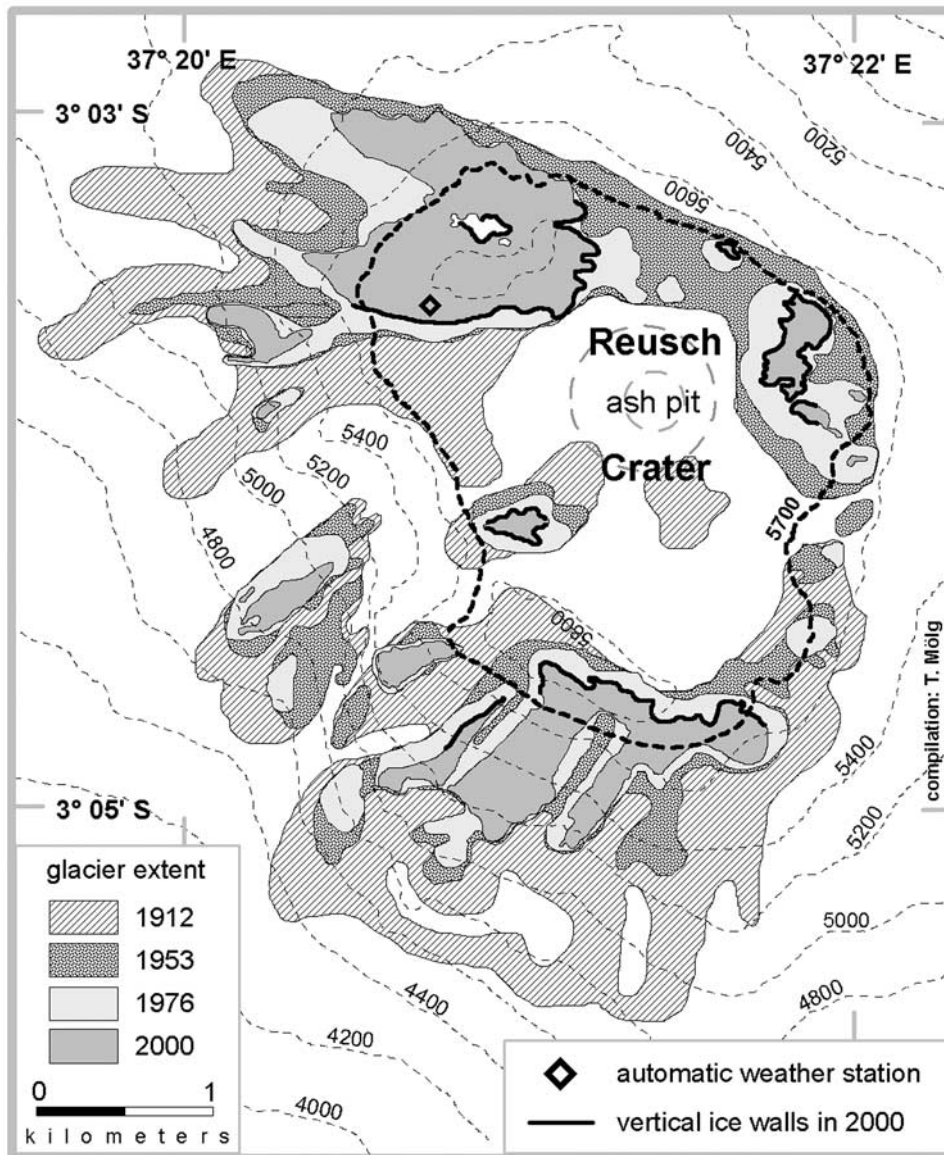


Figure 1. Glacier extents on Kibo in 1912, 1953, and 1976 after *Hastenrath and Greischar* [1997], and in 2000 after *Thompson et al.* [2002], and spatial distribution of vertical ice walls determined stereoscopically from air photos taken in February 2000 (map contours in meters, UTM zone 37 S projection). The highlighted 5,700 m-contour is a good indicator for delimiting the summit plateau. Dashed circles on this plateau depict the conical Reusch Crater with the ash pit opening. Map compiled by Thomas Mölg, January 2003.

account is necessary because interpreting climate fluctuations from glacier variations is a difficult exercise, especially in low latitudes [*Kaser, 2001*]. Thus *Kaser et al.* [2003] propose to define at least three different glacier regimes for investigating glacier recession on Kilimanjaro: (1) the summit horizontal glacier surfaces, (2) the summit vertical ice walls/cliffs, and (3) the slope glaciers below the summit. These regimes differ in mechanisms of energy and mass exchange at the ice-atmosphere interface, and the climatic controls behind them. A potential fourth regime of basal melting due to geothermal heat may have been effective only inside the RC - and may have helped to initiate glacier recession. On this basis, the dominant reason for the continuous glacier retreat on Kilimanjaro must be seen in atmo-

spheric conditions much drier than in a previous period when glaciers experienced growth. This view is consistent with glacier retreat on Mount Kenya and in the Rwenzori Range being dominately governed by the effects of a drier climate since ca. 1880 [*Kruss, 1983; Kruss and Hastenrath, 1987; Mölg et al., 2003*], as explained in section 1.

[7] This study undertakes a first step in using the concept presented by *Kaser et al.* [2003] and addresses the regime of the summit glaciers' vertical ice walls. These walls are primarily north- and south-facing, and typically form the margin of the summit glaciers, as illustrated by Figure 1 for the 2000-extent, and they have suffered continuous lateral retreat during the 20th century [*Thompson et al., 2002*]. This implies (1) the occurrence of persistent negative mass

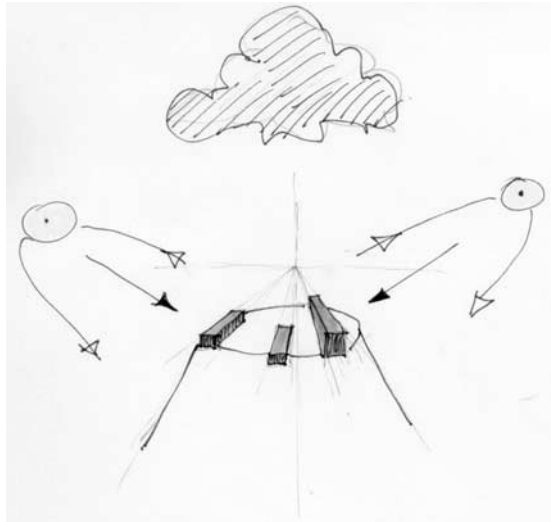


Figure 2. Concept of seasonal variations of the effective solar incidence on Kilimanjaro after *Kaser et al.* [2003] during dry seasons (Sun is north or south of the equator) and rainy seasons (Sun is approximately at zenith over equatorial latitudes). See color version of this figure at back of this issue.

balances on these walls, and (2) that ablation is mainly tied to solar radiation (i.e., energy flux from net shortwave radiation) and its unique geometry in the tropics, which is additionally supported by the strong east-west orientation of all remaining ice bodies (Figure 1). Consideration (2) can be clarified when looking at the other basic terms of the energy balance of a snow/ice surface. A positive energy flux from both net longwave radiation and sensible heat must be ruled out from a physical viewpoint, due to the observed pattern of differential ablation [*Kraus*, 1972] and consistently negative air temperature as measured at the AWS (February 2000–July 2002). The third remaining term, sublimation (i.e., turbulent latent heat flux), is another potential ablation mechanism but is too energy consuming to dominate strongly negative mass balance regimes [e.g., *Kuhn*, 1990] and thus the observed retreat of the ice walls. The conceptual model for the retreat of the vertical ice walls on the summit after *Kaser et al.* [2003] is depicted in Figure 2. During intensified dry seasons (solstitial periods), the vertical cliffs are alternately exposed to substantial solar radiation-driven ablation (i.e., north-facing during boreal summer, south-facing during austral summer), while summit glacier bodies are protected from the direct sun during the rainy seasons (equinoctial periods) through clouds. This study’s aim is to evaluate the role of solar radiation in controlling the retreat of the vertical ice walls on Kibo and thus maintaining glacier recession on the summit in the drier climate since ca. 1880. In the present absence of specific measurements directly at the ice walls, the study relies on a primarily qualitative, exploratory approach.

3. Combined Ice-Radiation Geometry Modeling

[8] To test the radiation hypothesis, a process-based model was designed, consisting of an idealized 1880-ice cap model (section 3.1) and a radiation model (section 3.2).

The combination of these two (section 3.3) provides a tool which isolates the following process: mass exchange at the vertical ice walls, between 1880 and 2000, as a function of energy available solely from solar radiation. Other energy sources potentially influencing ice ablation on the walls are not explicitly resolved in the model, but discussed in section 5.

3.1. The Ice Cap Model

[9] Since it is believed that Kibo’s summit ice cap was closed before the onset of glacier recession around 1880 [e.g., *Humphries*, 1959], the idealized 1880-ice cap model is a cylinder 2,400 m in diameter that fills the summit plateau. A smaller cylinder 800 m across is cut out at the center, representing the RC which was already free of ice when the first researchers reached the summit in the late 1880s [*Meyer*, 1900], most probably due to volcanic fumarole activity which has been documented since 1933 [e.g., *Tilman*, 1937; *Spink*, 1944]. The height of the cylinder is set to 50 m since this is a realistic average height for the ice walls as estimated by early researchers [e.g., *Meyer*, 1900; *Klute*, 1920]. Figure 3 shows ground plane and profile views of the 1880-ice cap model. The lines drawn in the ground plane (Figure 3a) reveal the discretization of the ice cap into 75 polygons, each margined by a vertical wall on

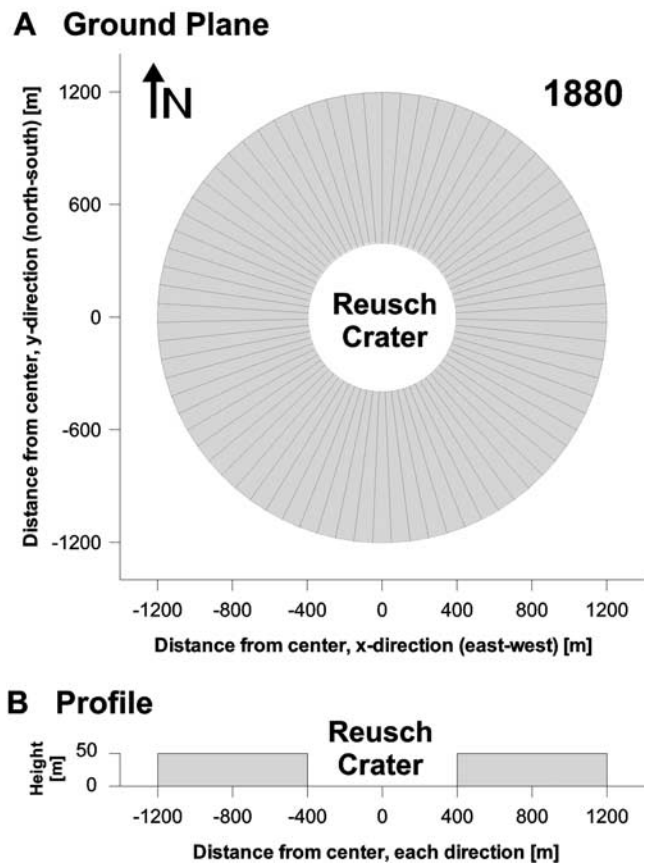


Figure 3. (a) Ground plane and (b) profile of the idealized 1880-ice cap that is completely margined by vertical walls. Lines in the ground plane show the discretization of the ice cap into 75 uniform polygons (in a 2-D view). Vertical scale of the profile depicted at three times horizontal.

its outer rim (99.95 m in width in the ground plane) and inner rim (33.5 m in width), as illustrated by the profile (Figure 3b). In aspect, each vertical wall always differs by 4.8° with respect to its neighboring walls. The exact spatial distribution of Kibo's summit vertical ice walls has not been mapped before 2000 (Figure 1). Shortly after the onset of glacier recession, vertical ice walls are well documented for the inner margin of the summit ice cap but only for the east of the outer margin in Meyer's [1900] book. This limited information justifies the uniformly vertical margin assumed for the entire ice cap model. Furthermore, the wall of each discrete polygon has homogenous surface characteristics.

3.2. The Radiation Model

[10] To compute the energy flux from solar radiation on the idealized ice cap's vertical walls, a modified version of the radiation model used by Hastenrath [1984], Kruss and Hastenrath [1987] and Hastenrath and Greischar [1997] to model shortwave radiation on Mount Kenya and Kilimanjaro was applied. Hastenrath [1984] verified this radiation model on nearby Mount Kenya. The modified version was recently applied to the Rwenzori Range [Mölg, 2002; Mölg et al., 2003] and is completely summarized in Mölg et al. [2003]. Its basic element is the formula for calculating clear-sky direct solar radiation on a planar surface $SW\downarrow(dir)$:

$$SW\downarrow(dir) = S_0 E_0 \cos \zeta_p \left[\frac{0.907}{(\sin h)^{0.018}} \right]^{\frac{T}{\sin h}} \quad (1)$$

S_0 is the solar constant with a standard value of $1,370 \text{ W m}^{-2}$, E_0 is the eccentricity correction factor, that is the square of the ratio of mean to true distance of the sun, ζ_p is the zenith angle of the sun with respect to an arbitrarily oriented and inclined plane (i.e., arbitrarily oriented vertical walls for this study), h is solar elevation above the plane of the horizon, and T is the so-called "Linke turbidity factor". Geometrical formulas for calculating E_0 , ζ_p , and h are to be found in classical books on the physics of solar radiation [e.g., Robinson, 1966; Iqbal, 1983]. Note that the formula for gaining the cosine of ζ_p can be reduced in the case of vertical walls, which is shown by Iqbal [1983]. The turbidity factor T , which is an indicator of water vapor and haze in the air [Robinson, 1966], was determined from monthly mean values of water vapor pressure measured at the AWS between February 2000 and June 2002, using the expression initially given by Bernhardt and Philipps [1958]. As expected, the turbidity factor at such a high altitude varies little during a year. Nevertheless, the annual cycle of turbidity on Kibo reflects the annual cycle of moisture very well (Figure 4), apart from January, which can be explained by the fact that January 2001 was one of the wettest for decades in the East African region [Waple et al., 2002]. The twelve monthly values for T obtained from the AWS data were assumed to be representative for all the years of the calculation period, 1880–2000, since no major changes in air humidity have been reported since the end of the 19th century [Hastenrath, 2001]. In addition, formula (1) is not particularly sensitive to T , as analyzed by Hastenrath [1984]. Uncertainties in T of $\pm 10\%$ induce changes of $< 2\%$ in monthly mean values of modeled direct solar radiation. Such an uncertainty of 2% would alter the speed of ice wall

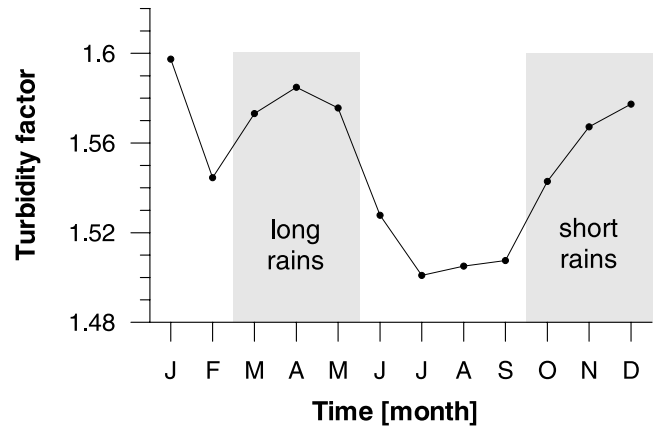


Figure 4. Annual cycle of turbidity on Kibo (monthly means) calculated from AWS data from February 2000 to June 2002 with the expression initially provided by Bernhardt and Philipps [1958]. Grey rectangles indicate the periods of the two rainy seasons schematically [Coutts, 1969; Basalirwa et al., 1999]. The turbidity factor is a dimensionless value, which is explained in detail by, e.g., Becker [2001].

retreat in the model by only 4 to 11 m in 120 years (referring to the monthly means of solar radiation on ice walls in scenario A, see section 4). These dimensions are negligible compared to the initial size of the model ice cap (2,400 m in diameter).

[11] The diffuse fraction of solar radiation under clear-sky was not included in the calculations, since direct solar radiation represents ca. 95% of clear-sky incoming short-wave radiation, as measured on Mount Kenya [Hastenrath, 1984]. Also, parameterizations for diffuse radiation require many input data without being very accurate [e.g., Becker, 2001]. When incorporating cloudiness, formula (1) was multiplied with the term $(1 - kC)$, where k symbolizes an empirical coefficient (0.65 at the equator) and C cloudiness in tenths [Budyko, 1974; Hastenrath, 1984].

3.3. Combination and Model Settings

[12] The combined ice cap-radiation model basically operates in three steps. (1) Solar radiation on the vertical walls is computed for every day between 6.15 and 17.45 true local time (TLT) with a temporal resolution of 30 min, incorporating cloudiness as prescribed by the respective scenario, atmospheric turbidity for the respective month, and shading relative to the sun's position. (2) The annual mean of the energy flux from solar radiation is converted into annual ablation amounts for each vertical wall as a function of albedo, assuming that the energy available is entirely applied to melt and, thus, sublimation in the model is nil. Melting dominates ablation on the illuminated parts of the vertical walls, as reported by Kaser et al. [2003], which is consistent with the physical framework of Kuhn [1987] who showed that ice/snow may melt at air temperatures as low as -10°C , and furthermore with ablation studies on vertical ice walls in Antarctica [Lewis et al., 1999] (see section 5 for a detailed discussion). For this step (2), the model uses standard values for the heat constant for fusion $L_M = 0.334 \text{ MJ kg}^{-1}$, and for ice density $\rho_i =$

900 kg m⁻³ [e.g., Paterson, 1994]. (3) The new spatial extent and geometry of the ice cap, and its new glacier surface area for various points in time after 1880 are calculated, i.e., every polygon of the ice cap model (in a 2-D view) retreats individually on its inner and outer margin within the set time step. Since summit ice bodies do not indicate any dynamics, ice flow is neglected, as well as accumulation (i.e., resublimation: direct transition of water from vapor to solid phase) on the vertical walls [Kaser et al., 2003].

[13] Because this study does not address the glacier regime of the summit horizontal glacier surfaces, the long-term mass balance on the horizontal surface of the ice cap model is assumed to be 0, so no surface lowering occurs in the model. This might be true until ca. 1960, but not for the more recent decades which involved increased negative mass balance frequency [Hastenrath and Greischar, 1997; Thompson et al., 2002]. However, surface lowering of the summit ice bodies since the 1960s of course induced changes in glacier volume, but lowering was not strong enough to contribute decisively to glacier surface area change [Kaser et al., 2003], and this latter parameter is used to finally validate the model results (section 4).

[14] Since the single polygons building the ice cap retreat differentially, and produce additional artificial edges on the inner and outer ice cap margin, the idea arose to smooth the margins after each constant time step with a smoothing algorithm. To optimally smooth the margins, the algorithm we developed alters the aspect of the vertical walls, which affects the cosine of ζ_p in formula (1) [e.g., Iqbal, 1983]. However, calculated time series of the ice cap model's glacier surface area (1880–2000) in a prescribed scenario A (see section 4 below) showed that values only differ in the dimension 10⁻² after 120 years between the runs with and without smoothing, regardless of whether a small (e.g., 5 years) or large time step (e.g., 30 years) was chosen. Therefore on the basis of this sensitivity analysis of edge effects, the complex smoothing algorithm was not taken into consideration for further calculations.

4. Results

[15] In a first scenario A, the combined model was solely forced with an annual cycle of clouds and with an albedo on the vertical ice walls $a_w = 0.5$ (albedo value selection is discussed further below). Regarding cloudiness, the March–May and October–December rainy seasons were assumed to be completely cloud-covered all day ($C = 10/10$), and the two dry seasons in January/February and from June to September were treated as all-day clear sky. This choice of the largest possible difference in C between dry and rainy seasons must be understood as a first schematic approximation. The differentiation of hygric seasons is based on the work of Coutts [1969] who first performed a detailed quantitative analysis of the temporal and spatial distribution of rainfall in the Kilimanjaro region. His results were confirmed by the more recent study of Basalirwa et al. [1999] who used long-time precipitation records of Tanzania (1961–1990) for a principal component analysis (PCA). Figure 5 shows the results for scenario A, where the combined model output is displayed in 30-year intervals. Two decisive aspects emerge from this simple scenario A.

(1) Two big ice bodies detach from the formerly closed ice cap and remain north and south of RC, which indicates the formation of the Northern and Southern Icefields. (2) These remaining ice bodies have a well pronounced east-west orientation. Initially, scenario A was forced with an albedo $a_w = 0.6$, but the opening in the east and west of the idealized ice cap then occurs too late (after 1970), so a_w was decreased to 0.5 (“speed adjustment”) which is, probably, a bit too low for the brightly appearing ice walls. This discloses that albedo is a tuning parameter in the model, not only describing the reflection of solar radiation on the ice walls, but additionally parameterizing other factors such as uncertainties due to the simplified cloud forcing (i.e., the value of C). Thus changing the values of C and a_w in scenario A only affects the speed, but not the spatial pattern of ice recession - which is an exclusive product of solar radiation geometry. For this scenario A, the idealized summit ice cap would have completely disappeared in the model year 2046.

[16] Since scenario A's calculations yield a quite clear result, a second scenario B including three mountain-characteristic, climate-related phenomena was run to check the initial result's expressiveness. All three phenomena rely on observational evidence and can be parameterized qualitatively by modifying the two model-forcing variables, cloudiness and albedo. Again, solar radiation is the only driving energy flux in the model. The three phenomena are as follows. (1) The retreat of ice walls on the outer margin of the idealized ice cap is suppressed (i.e., $a_w = 1$) in the south and northwest sectors (160° to 200°, and 290° to 340°; clockwise), since no vertical walls currently exist in these areas where slope glaciers connect with the summit ice bodies, as the map shows (Figure 1). Thus a lateral ice retreat did not take place in these parts throughout the period of interest, 1880–2000. (2) The albedo on ice walls of the outer margin is increased to 0.75 in the east-north-east sector (between 45° and 90°; clockwise) and the southwest sector (between 200° and 250°; clockwise) in order to account for the advection of relatively moist air, as reflected in the spatial distribution of annual precipitation with two maxima in these aspects of the mountain [Coutts, 1969]. Advection of moist air leads to formation of hoar frost on objects facing the flow of the moist air mass, a typical and well-known process in mountain meteorology [e.g., Liljequist and Cehak, 1994; Whiteman, 2000], and one we observed on Kibo. In the combined model, the higher albedo not only expresses increased reflectivity of solar radiation on the affected ice walls but again parameterizes other factors, e.g., changed small-scale cloud conditions in this case. (3) A diurnal cycle of convective clouds is included in the dry season months (10/10 cloud cover from 15.00 TLT on). This characterizing process for tropical high mountains was nicely discussed earlier by Spink [1945] for Kilimanjaro, and first described in detail by Troll and Wien [1949] for nearby Mount Kenya. It has been taken into consideration and re-described in more recent model studies on glacierized tropical mountains by Kaser and Georges [1997], Hastenrath and Greischar [1997], and Mölg et al. [2003]. Hastenrath [1991] provides a detailed, explicit view on this process. Scenario B's results for the year 2000 are depicted in Figure 6. A smaller Eastern Icefield has formed and separated away from the Northern Icefield which is now

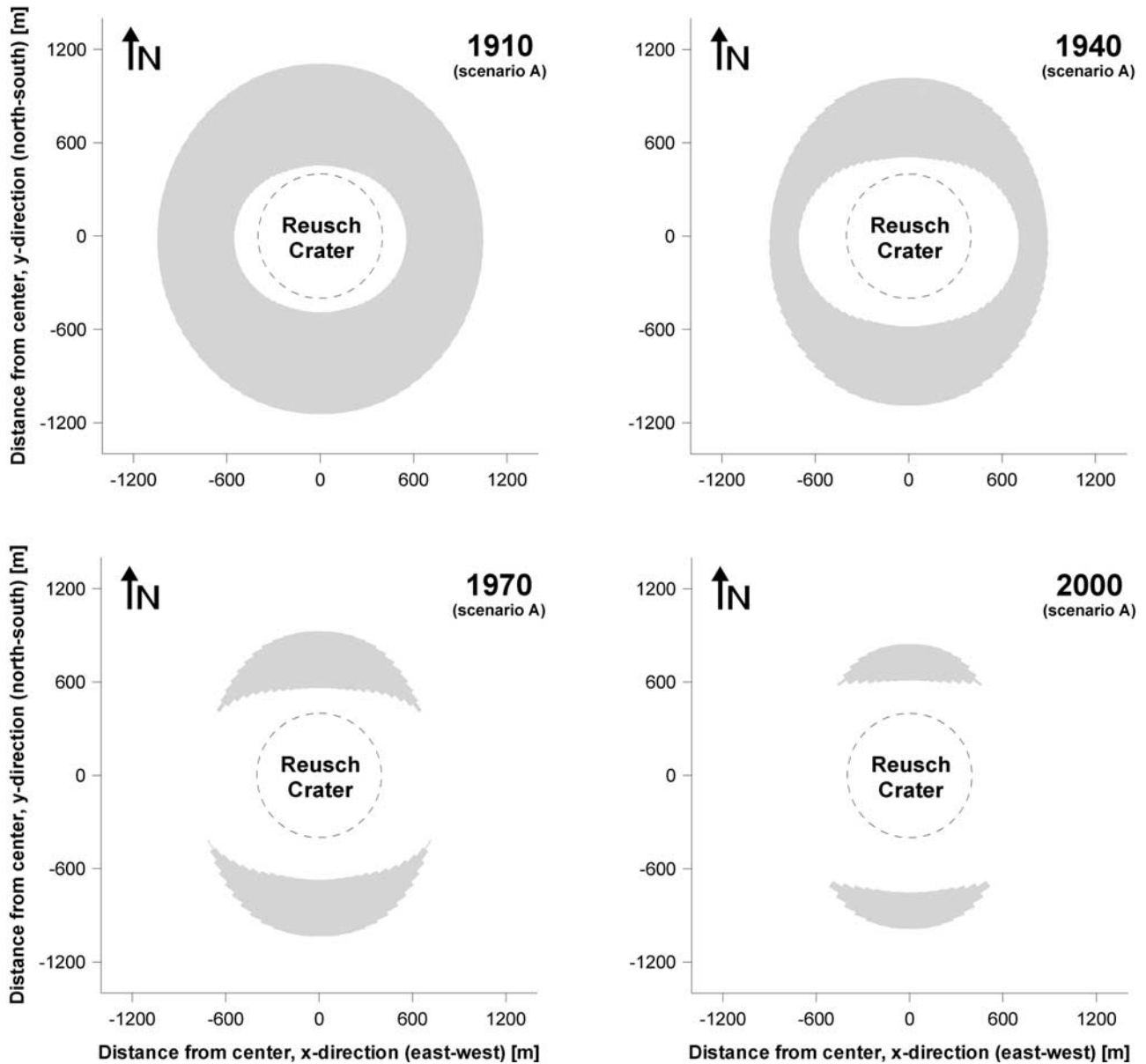


Figure 5. Spatial pattern of the idealized ice cap's glacier surface area in 1910, 1940, 1970, and 2000, as calculated from the combined ice-radiation geometry model for a prescribed scenario A (scenario properties see text).

concentrated more northwest of RC. The Southern Icefield remains quite stable south of RC.

5. Discussion

[17] Although the modeled pattern of ice retreat on Kibo nicely indicates that observed, several questions and issues need to be discussed further; each is given one paragraph in the section below.

[18] Why are the remaining ice bodies concentrated more closely to the summit plateau's outer margin in reality than indicated by the model (cf. bold dashed lines in Figure 6 and Figure 1)? This question most probably requires looking at two processes, one on the outer margin, and another on the inner margin of the real ice cap. For the outer ice margin, the spatial distribution of

vertical walls might be decisive. These walls are explicitly reported only to the east of the summit plateau (i.e., southeast of RC) before 1900 [Meyer, 1900]. When, or if, vertical walls were formed in the remaining sectors is not clear, since Figure 1 represents the first mapping of these features. Viewing the present northwest and south sectors in Figure 1 illustrates that the lateral ice retreat is rarely pronounced where these walls are absent. Consequently, the model overestimates ice retreat on the outer margin due to the assumption of widespread vertical ice walls in the initial conditions (i.e., 1880). Running the model with partly inclined edges is not possible at the current stage, since this would require more empirical data and knowledge on the mass and energy balance of horizontal ice surfaces and slope glaciers. On the inner ice margin, the additional energy from the horizontal

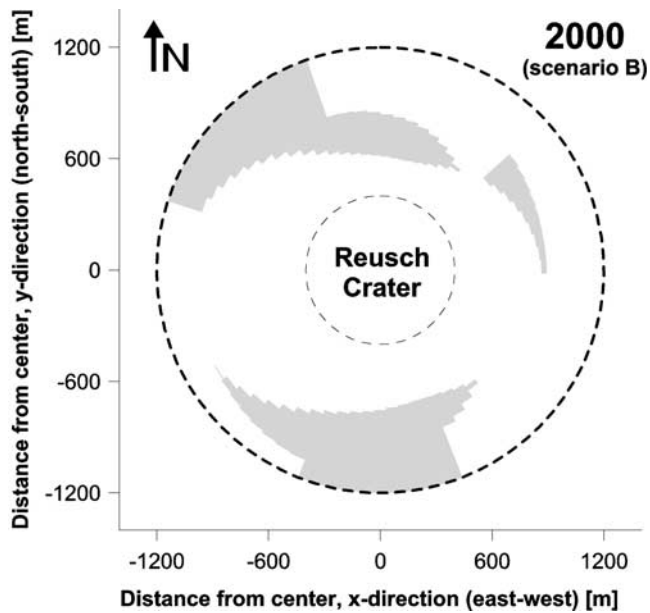


Figure 6. Spatial pattern of the idealized ice cap's glacier surface area in 2000, as calculated from the combined ice-radiation geometry model for a prescribed scenario B (scenario properties see text). The bold dashed circle indicates the initial 1880-ice cap's outer margin.

summit plateau's outgoing longwave radiation flux $L\uparrow_p$ seems a reasonable explanation for an intensified ice retreat on the inner margin, since solar radiation received at the plateau surface and its outgoing longwave radiation flux certainly show a direct, temporally consistent proportionality. $L\uparrow_p$ might be especially effective during the dry season when snow rarely covers the plateau's dark ashes, and considerable solar energy is absorbed. That heating of the dark ashes becomes just as effective for ice wall ablation through the turbulent sensible heat flux (i.e., a turbulent energy transfer from locally rising warm air toward the ice wall surface) seems unlikely. The main argument for this is found in the peculiar microclimate directly at the ice wall, which is characterized by low wind speeds that reduce turbulent heat exchange drastically. This microclimate was described in more detail by Kaser *et al.* [2003] and is also present at vertical ice walls of Antarctic glaciers [Lewis *et al.*, 1999], which is discussed further just below with regard to sublimation and its relevance for ice wall retreat. However, a detailed evaluation of the role of heated plateau ashes in forcing ablation on the inner ice walls, especially by $L\uparrow_p$, will require specific field measurements and specific micrometeorological simulations.

[19] In connection with the discussion above, the formation of vertical ice walls on Kibo summit in general represents an open question. While mechanical processes seem to dominate the formation process of vertical ice walls in high latitudes [e.g., Hooke, 1970], calving of the ice cliffs on Kibo is probably of minimal importance, as reported by Kaser *et al.* [2003] who present a qualitative interpretation of ice cliff formation on the mountain. Quantitative dimensions of energy fluxes and/or mechanical processes involved in this formation remain unclear. The existence

of the latter is questionable, since summit ice bodies do not show any apparent evidence of ice dynamics, as mentioned in the context of model assumptions (section 3.3). From a physical perspective, the little thickness of the summit glaciers scarcely enables internal deformation, and the planar summit plateau prevents basal sliding in response to gravity.

[20] How important is sublimation for vertical ice wall ablation? This second heat-consuming ablation process besides melting is, most probably, of minimal importance at the ice walls. In addition to our field observations of strong melting [Kaser *et al.*, 2003], the energy balance studies of Chinn [1987] and Lewis *et al.* [1999] in Antarctica point to this fact. These studies were performed in a very similar microclimatic setting (dry and cold conditions) and on a glacier with vertical edges and a horizontal surface (Canada Glacier). Their analyses highlight that the majority (2/3 and more) of available energy at the glacier's vertical terminus cliff is consumed by melting (primarily enabled due to low wind speeds), which causes strong ablation. In contrast, sublimation dominates ablation on the horizontal surface of Canada Glacier, consuming ca. 90% of available energy. This predominance of sublimation in governing ablation is also expected on the horizontal ice surfaces on Kibo summit, which are exposed to the strong gradient wind, favouring turbulent exchange of latent heat. For vertical ice wall ablation on Kibo, however, sublimation can be neglected in this model study. Even if introducing sublimation into the model, e.g., through consuming a constant small rate of available energy, the speed of ice recession would have been affected exclusively. The resulting spatial pattern would not change.

[21] How did the small Furtwängler Glacier southwest of RC, the fourth ice entity on the summit, form? This process is not indicated by the combined model. From images of the www-server for the University of Massachusetts at <http://www.geo.umass.edu/climate/kibo.html>, it appears that this glacier occupies an area protected from radiation as a result of RC's topography. Especially in the months around the summer solstice (21 June; i.e., sun north of Kibo), a dry period promoting ablation, the morning sun's low incidence angle could produce a pronounced shaded area, favoring protection of Furtwängler Glacier. Since the model used in this study does not include the relief of Kibo summit, this may explain why Furtwängler Glacier could not be simulated. Thompson *et al.* [2002] also stress the exceptional position of Furtwängler and speculate that it is an ephemeral feature, unlike the larger ice fields. The relief of the mountain might also influence the configuration of the Southern Icefield which is "blocked" by the well pronounced ridge harboring the highest point, Uhuru Peak (5,895 m). This ridge is indicated by the 5,800 m-contour in Figure 1 and explains why the Southern Icefield could never extend closer to RC during the 20th century.

[22] What precise role does the temporal and spatial distribution of cloudiness on the mountain play? Cloudiness was primarily treated qualitatively in this study, following the basic temporal distribution of rains [Coutts, 1969; Basalirwa *et al.*, 1999] and classical descriptive models [Troll and Wien, 1949]. Monitoring the exact annual

and diurnal cycles of cloudiness, and the respective spatial patterns, would provide (1) more accurate input to the model presented here (i.e., improving modeling shortwave radiation), and (2) a necessary parameter for future studies trying to reproduce real changes in Kibo's glaciation. Such studies would have to consider other energy fluxes in addition to solar radiation. In this context, the energy flux from incoming longwave radiation is especially important, as this term greatly depends on cloudiness, and thus experiences a pronounced seasonality in tropical climate, as *Francou et al.* [2003] discuss for a tropical glacier in the Bolivian Andes. Monitoring cloudiness might be done, in the best case, with a network of radiometers or light meters. Currently, there are too sparse data to model the spatial distribution of incoming longwave radiation on the mountain.

6. Conclusions and Perspective

[23] In the light of understanding the climatological basis for glacier recession on Kilimanjaro, this study addresses the glacier regime of the summit vertical ice walls/cliffs, and provides a clear indication that solar radiation is the main climatic parameter governing and maintaining ice retreat on the mountain's summit plateau in the drier climate since ca. 1880. This principal conclusion is based on the results drawn from a process-based model combining ice-radiation geometry, a model specifically designed for Kilimanjaro's glacier-climate environment. Model results also indicate that retreat on the inner ice cap margin was supported by an additional energy source, most probably outgoing longwave radiation from the dark-ash covered summit plateau. Following this indication, additional measurements at the summit ice walls are suggested, in order to improve the model used in this study with regard to complexity, and to detect the other climatic parameters involved in the retreat process quantitatively by analyzing all the main terms in the ice wall's surface energy balance. Additional measurements and further modeling are absolutely necessary to understand Kilimanjaro's glacier retreat, and associated changes in the diverse temporal and spatial scales of the climate system more completely.

[24] Solar radiation as one driving force of glacier recession on Kilimanjaro agrees with the findings of *Kruss and Hastenrath* [1987] and *Mölg et al.* [2003] who showed that incoming shortwave radiation is an essential contributor to ice recession on the two other glacierized massifs of East Africa, Mount Kenya and Rwenzori, since the end of the 19th century. This strong radiation effect on glacier retreat is understood as a direct consequence of the 20th century dry East African climate with a lack of accumulation, allowing the mass balance of the glaciers to be dominated by ablation that, in turn, is enhanced by greater net shortwave radiation due to decreased cloudiness. Moreover, this study highlights that modern glacier retreat on Kilimanjaro is much more complex than simply attributable to "global warming only", a finding that conforms with the general character of glacier retreat in the global tropics [*Kaser*, 1999]: a process driven by a complex combination of changes in several different climatic parameters [e.g., *Kruss*, 1983; *Kruss and Hastenrath*, 1987; *Hastenrath and Kruss*, 1992;

Kaser and Georges, 1997; *Wagnon et al.*, 2001; *Kaser and Osmaston*, 2002; *Francou et al.*, 2003; *Mölg et al.*, 2003], with humidity-related variables dominating this combination.

[25] **Acknowledgments.** The Kibo automatic weather station program is funded by grant ATM-9909201 to the University of Massachusetts from the U.S. NSF Paleoclimate Program. Thomas Mölg would like to thank the Theodor-Körner-Foundation (Vienna) for supporting this research. The comments and suggestions of Stefan Hastenrath and two anonymous reviewers nicely improved this manuscript.

References

- Alverson, K., R. Bradley, K. Briffa, J. Cole, M. Hughes, I. Larocque, T. Pedersen, L. G. Thompson, and S. Tudhope, A global paleoclimate observing system, *Science*, 293, 47–49, 2001.
- Basalirwa, C. P. K., J. O. Odiyo, R. J. Mingodo, and E. J. Mpetta, The climatological regions of Tanzania based on the rainfall characteristics, *Int. J. Climatol.*, 19, 69–80, 1999.
- Becker, S., Calculation of direct solar and diffuse radiation in Israel, *Int. J. Climatol.*, 21, 1561–1576, 2001.
- Bernhardt, F., and H. Philipps, *Die Räumliche und Zeitliche Verteilung der Einstrahlung, der Ausstrahlung und der Strahlungsbilanz im Meeresniveau, teil 1, Die Einstrahlung*, Meteorol. und Hydrol. Dienst der DDR, Berlin, 1958.
- Budyko, M. I., *Climate and Life*, Academic, New York, London, 1974.
- Chinn, T. J. H., Accelerated ablation at a glacier ice-cliff margin, dry valleys, Antarctica, *Arct. Alp. Res.*, 19, 71–80, 1987.
- Coutts, H. H., Rainfall of the Kilimanjaro area, *Weather*, 24, 66–69, 1969.
- Downie, C., and P. Wilkinson, *The Geology of Kilimanjaro*, Dept. of Geology, Sheffield Univ., Sheffield, UK, 1972.
- Francou, B., M. Vuille, P. Wagnon, J. Mendoza, and J. E. Sicart, Tropical climate change recorded by a glacier in the central Andes during the last decades of the 20th century: Chacaltaya, Bolivia, 16°S, *J. Geophys. Res.*, 108(D5), 4059, doi:10.1029/2002JD002473, 2003.
- Geilinger, W., The retreat of the Kilimanjaro glaciers, *Tanganyika Notes Rec.*, 2, 7–20, 1936.
- Georges, C., and G. Kaser, Ventilated and unventilated air temperature measurements for glacier-climate studies on a tropical high mountain site, *J. Geophys. Res.*, 107(D24), 4775, doi:10.1029/2002JD002503, 2002.
- Griffiths, J. F., *Climates of Africa*, Elsevier Sci., New York, 1972.
- Hardy, D. R., M. Vuille, C. Braun, F. Keimig, and R. S. Bradley, Annual and daily meteorological cycles at high altitude on a tropical mountain, *Bull. Am. Meteorol. Soc.*, 79, 1899–1913, 1998.
- Hastenrath, S., *The Glaciers of Equatorial East Africa*, D. Reidel, Norwell, Mass., 1984.
- Hastenrath, S., *Climate Dynamics of the Tropics*, Kluwer Acad., Norwell, Mass., 1991.
- Hastenrath, S., Glacier recession on Mount Kenya in the context of the global tropics, *Bull. Inst. Fr. Études Andines*, 24, 633–638, 1995.
- Hastenrath, S., Variations of East African climate during the past two centuries, *Clim. Change*, 50, 209–217, 2001.
- Hastenrath, S., and L. Greischar, Glacier recession on Kilimanjaro, East Africa, 1912–89, *J. Glaciol.*, 43, 455–459, 1997.
- Hastenrath, S., and P. D. Kruss, The dramatic retreat of Mount Kenya's glaciers between 1963 and 1987: Greenhouse forcing, *Ann. Glaciol.*, 16, 127–133, 1992.
- Hastenrath, S., R. Rostom, and R. A. Caukwell, Variations of Mount Kenya's glaciers 1963–87, *Erdkunde*, 43, 202–210, 1989.
- Hay, S. I., J. Cox, D. J. Rogers, S. E. Randolph, D. I. Stern, G. D. Shanks, M. F. Myers, and R. W. Snow, Climate change and the resurgence of malaria in the East African highlands, *Nature*, 415, 905–909, 2002.
- Hooke, R. L., Morphology of the ice-sheet margin near Thule, Greenland, *J. Glaciol.*, 9, 303–324, 1970.
- Humphries, D. W., Preliminary notes on the glaciology of Kilimanjaro, *J. Glaciol.*, 3, 475–478, 1959.
- Hunt, T. L., Weather conditions on Kilimanjaro, *Weather*, 2, 338–344, 1947.
- Intergovernmental Panel on Climate Change, *Climate Change 2001: The Scientific Basis*, Cambridge Univ. Press, New York, 2001.
- Iqbal, M., *An Introduction to Solar Radiation*, Academic, Toronto, New York, London, 1983.
- Irion, R., The melting snows of Kilimanjaro, *Science*, 291, 1690–1691, 2001.
- Jäger, F., Veränderungen der Kilimanjaro-Gletscher, *Z. Gletscherk.*, 19, 285–299, 1931.
- Kaser, G., A review of the modern fluctuations of tropical glaciers, *Global Planet. Change*, 22, 93–103, 1999.

- Kaser, G., Glacier-climate interaction at low latitudes, *J. Glaciol.*, 47, 195–204, 2001.
- Kaser, G., and C. Georges, Changes in the equilibrium line altitude in the tropical Cordillera Blanca (Perú) between 1930 and 1950 and their spatial variations, *Ann. Glaciol.*, 24, 344–349, 1997.
- Kaser, G., and B. Noggler, Glacier fluctuations in the Rwenzori Range (East Africa) during the 20th century: A preliminary report, *Z. Gletscherk. Glazialgeol.*, 32, 109–117, 1996.
- Kaser, G., and H. Osmaston, *Tropical Glaciers*, Cambridge Univ. Press, Cambridge, 2002.
- Kaser, G., S. Hastenrath, and A. Ames, Mass balance profiles on tropical glaciers, *Z. Gletscherk. Glazialgeol.*, 32, 75–81, 1996.
- Kaser, G., D. R. Hardy, T. Mölg, and R. S. Bradley, Modern glacier retreat on Kilimanjaro as evidence of climate change: Observations and facts, *Int. J. Climatol.*, in press, 2003.
- King'uyu, S. M., L. A. Ogallo, and E. K. Anyamba, Recent trends of minimum and maximum surface temperatures over Eastern Africa, *J. Clim.*, 13, 2876–2886, 2000.
- Klute, F., *Ergebnisse der Forschungen am Kilimandscharo 1912*, Reimer-Vohsen, Berlin, 1920.
- Kraus, H., Energy exchange at air-ice interface, *IAHS Publ.*, 107, 128–164, 1972.
- Kruss, P. D., Climate Change in East Africa: A numerical simulation from the 100 years of terminus record at Lewis Glacier, Mount Kenya, *Z. Gletscherk. Glazialgeol.*, 19, 43–60, 1983.
- Kruss, P. D., and S. Hastenrath, The role of radiation geometry in the climate response of Mount Kenya's glaciers, part 1: Horizontal reference surfaces, *Int. J. Climatol.*, 7, 493–505, 1987.
- Kuhn, M., Micro-meteorological conditions for snow melt, *J. Glaciol.*, 33, 24–26, 1987.
- Kuhn, M., Energieaustausch Atmosphäre-Schnee und Eis, in *Schnee, Eis und Wasser der Alpen in einer wärmeren Atmosphäre*, edited by D. Vischer, pp. 21–32, Versuchsanst. für Wasserb., Hydrol. und Glaziol., Zürich, Switzerland, 1990.
- Lewis, K. J., A. G. Fountain, and G. L. Dana, How important is cliff melt?: A study of the Canada Glacier terminus, Taylor Valley, Antarctica, *Global Planet. Change*, 22, 105–115, 1999.
- Liljequist, G. H., and K. Cihak, *Allgemeine Meteorologie*, 3rd ed., Vohsen, Braunschweig, Germany, 1994.
- Meyer, H., *Der Kilimandscharo*, Reimer-Vohsen, Berlin, 1900.
- Mölg, T., Modellierung der kurzwelligen Einstrahlung mit GIS am Beispiel eines tropischen Hochgebirges, in *Beiträge zum AGIT-Symposium Salzburg 2002*, edited by J. Strobl, T. Blaschke, and G. Griesebner, pp. 347–356, Wichmann-Verlag, Heidelberg, Germany, 2002.
- Mölg, T., C. Georges, and G. Kaser, The contribution of increased incoming shortwave radiation to the retreat of the Rwenzori Glaciers, East Africa, during the 20th century, *Int. J. Climatol.*, 23, 291–303, 2003.
- Nicholson, S. E., and X. Yin, Rainfall conditions in Equatorial East Africa during the nineteenth century as inferred from the record of Lake Victoria, *Clim. Change*, 48, 387–398, 2001.
- Oerlemans, J., *Glaciers and Climate Change*, Balkema, Lisse, 2001.
- Osmaston, H., Glaciers, glaciations and equilibrium line altitudes on Kilimanjaro, in *Quaternary and environmental Research on East African Mountains*, edited by W. C. Mahaney, pp. 7–30, A. A. Balkema, Brookfield, Vt., 1989.
- Paterson, W. S. B., *The Physics of Glaciers*, 3rd ed., Oxford Univ. Press, New York, 1994.
- Robinson, N., *Solar Radiation*, Elsevier Sci., New York, 1966.
- Rodhe, H., and H. Virji, Trends and periodicities in East African rainfall, *Mon. Weather Rev.*, 104, 307–315, 1976.
- Spink, P. C., Weather and volcanic activity on Kilimanjaro, *Geogr. J.*, 103, 224–229, 1944.
- Spink, P. C., Further notes on the Kibo inner crater and glaciers of Kilimanjaro and Mount Kenya, *Geogr. J.*, 106, 210–216, 1945.
- Thompson, L. G., et al., Kilimanjaro ice core records: Evidence of holocene climate change in tropical Africa, *Science*, 298, 589–593, 2002.
- Tilman, H. W., *Snow on the Equator*, G. Bell and Sons, London, 1937.
- Troll, C., and K. Wien, Der Lewis Gletscher am Mount Kenia, *Geogr. Ann.*, 31, 257–274, 1949.
- Verschuren, D., K. R. Laird, and B. F. Cumming, Rainfall and drought in equatorial east Africa during the past 1,100 years, *Nature*, 403, 410–414, 2000.
- Wagnon, P., P. Ribstein, B. Francou, and J. E. Sicart, Anomalous heat and mass budget of Glacier Zongo, Bolivia, during the 1997/98 El Niño year, *J. Glaciol.*, 47, 21–28, 2001.
- Waple, A. M., et al., Climate Assessment for 2001, *Bull. Am. Meteorol. Soc.*, 83, S1–S62, 2002.
- Whiteman, C. D., *Mountain Meteorology: Fundamentals and Applications*, Oxford Univ. Press, New York, 2000.

D. R. Hardy, Climate System Research Center, Department of Geosciences, University of Massachusetts, Amherst, MA 01003-9297, USA.

G. Kaser and T. Mölg, Tropical Glaciology Group, Department of Geography, University of Innsbruck, Innrain 52, A-6020 Innsbruck, Austria. (thomas.moelg@uibk.ac.at)

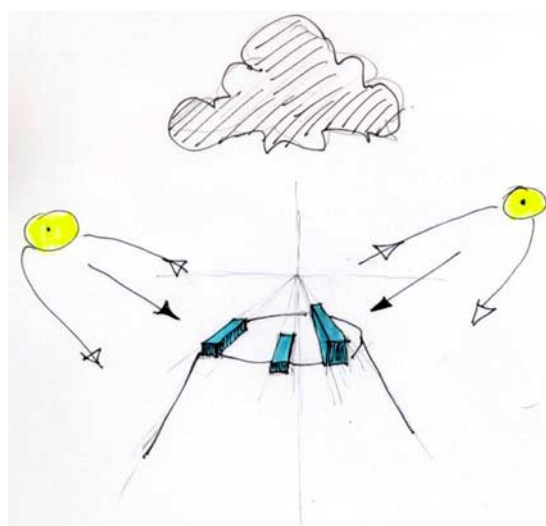


Figure 2. Concept of seasonal variations of the effective solar incidence on Kilimanjaro after *Kaser et al.* [2003] during dry seasons (Sun is north or south of the equator) and rainy seasons (Sun is approximately at zenith over equatorial latitudes).